Riemannian Anisotropic Diffusion for Tensor Valued Images

Kai Krajsek[1], Marion I. Menzel[1], Michael Zwanger[2], and Hanno Scharr[1]

[1] Forschungszentrum Jülich, ICG-3, 52425 Jülich, Germany
{k.krajsek,m.i.menzel,h.scharr}@fz-juelich.de
[2] Siemens AG, Healthcare Sector
MR Application Development, 91052 Erlangen, Germany
Michael.Zwanger@siemens.com

Abstract. Tensor valued images, for instance originating from diffusion tensor magnetic resonance imaging (DT-MRI), have become more and more important over the last couple of years. Due to the nonlinear structure of such data it is nontrivial to adapt well-established image processing techniques to them. In this contribution we derive anisotropic diffusion equations for tensor-valued images based on the intrinsic Riemannian geometric structure of the space of symmetric positive tensors. In contrast to anisotropic diffusion approaches proposed so far, which are based on the Euclidian metric, our approach considers the nonlinear structure of positive definite tensors by means of the intrinsic Riemannian metric. Together with an intrinsic numerical scheme our approach overcomes a main drawback of former proposed anisotropic diffusion approaches, the so-called *eigenvalue swelling effect*. Experiments on synthetic data as well as real DT-MRI data demonstrate the value of a sound differential geometric formulation of diffusion processes for tensor valued data.

1 Introduction

In this paper anisotropic diffusion driven by a diffusion tensor is adapted to tensor-valued data in a way respecting the Riemannian geometry of the data structure. *Nonlinear diffusion* has become a widely used technique with a well understood theory (see e.g. [1,2] for overviews). It was introduced in [3] and has been frequently applied to scalar-, color- or vector-valued data. *Anisotropic diffusion*[1] driven by a diffusion tensor [2] is the most general form of diffusion processes. *Tensor-valued data* frequently occur in image processing, e.g. covariance matrices or structure tensors in optical flow estimation (see e.g. [4]). Due to rapid technological developments in magnetic resonance imaging (MRI) also interest in tensor-valued measurement data increases. Due to the increasing need of processing tensor valued data, the development of appropriate regularization techniques become more and more important (e.g. see [5,6,7,8] and [9] as well as references therein). *Riemannian geometry* refers to the fact that the set of positive definite tensors $P(n)$ of size n does not form a vector space but a nonlinear manifold embedded in the vector space of all symmetric matrices. The nonlinear

[1] Please note that the term 'anisotropic diffusion' is not uniquely defined in literature. In this contribution we use the term in accordance with the definition given in [2].

D. Forsyth, P. Torr, and A. Zisserman (Eds.): ECCV 2008, Part IV, LNCS 5305, pp. 326–339, 2008.

structure of $P(n)$ is studied from a differential geometric point of view for a long time [10]. Due to the nonlinear structure of $P(n)$, well established image processing techniques for scalar and vector valued data might destroy the positive definiteness of the tensors. Approaches for processing tensor valued images can be classified into two groups: using extrinsic [5,11,12,13,14] or intrinsic view [15,16,17,18,19,20,21,7,22]. Methods using the extrinsic point of view consider the space of positive definite symmetric tensors as an embedding in the space of all symmetric tensors which constitute a vector space. Distances, as e.g. required for derivatives, are computed with respect to the flat Euclidian metric of the space of symmetric matrices. To keep tensors on the manifold of positive definite tensors, solutions are projected back onto the manifold [5], selected only on the manifold in a stochastic sampling approach [11], or processing is restricted to operations not leading out of $P(n)$, e.g. convex filters [12,13,14]. Although then tensors stay positive definite the use of a flat metric is not appropriate to deal with $P(n)$. For instance in regularization, the processed tensors become deformed when using the flat Euclidian metric [7] known as *eigenvalue swelling effect* [5,6,7,8]. Tschumperlé and Deriche [5] avoid the eigenvalue swelling effect by applying a spectral decomposition and regularizing eigenvalues and eigenvectors separatively. Chefd'hotel et al. [6] proposed to take the metric of the underlying manifold for deriving evolution equations from energy functionals that intrinsically fulfill the constraints upon them (e.g. rank or eigenvalue preserving) as well as for the numerical solution scheme. However, they consider the Euclidian metric for measuring distances between tensors such that their methods suffer from the eigenvalue swelling effect for some of the proposed evolution equations. Methods using the intrinsic point of view consider $P(n)$ as a Riemannian symmetric space (see [23] and Sect. 3 for an introduction in symmetric Riemannian spaces) equipped with an affine invariant metric on the tangent space at each point. Consequently, using this metric the eigenvalue swelling effect is avoided. The symmetry property of the Riemannian manifold easily allows to define evolution equations on the tangent spaces, approximate derivatives by tangent vectors as well as construct intrinsic gradient descent schemes as we will show for anisotropic diffusion in the following.

Related work. Differential geometric approaches have been introduced to different fields in image processing and computer vision [24,25,26]. Only quite recently, methods based on the Riemannian geometry of $P(n)$ have been introduced independently by different authors [16,17,18,19,20,21,7,22]. For instance, in [20,7] a 'Riemannian framework for tensor computing', has been proposed in which several well established image processing approaches including interpolation, restoration and isotropic nonlinear diffusion filtering have been generalized to $P(n)$ in an intrinsic way. Furthermore, an anisotropic regularization approach has been proposed by adapting the isotropic Laplace-Beltrami operator that can be identified with a second order Markov Random field approach. A quite similar approach has been proposed in [27] by formulating diffusion filtering directly on a discrete graph structure. In [8], a weighted mean has been proposed that allows to smooth the image in an anisotropic way. However, all these approaches [7,27,8], do not allow to construct diffusion tensors from model based structure estimation, as common in literature for scalar data [2]. To do so in an intrinsic way, one cannot do without a numerical scheme for mixed second order derivatives,

first introduced in the current paper. A computational more efficient approach than the framework of Pennec et al. [7] based on the so called *log-Euclidean* metric has been introduced in [28]. There, the positive definite tensors are mapped onto the space of symmetric matrices by means of the matrix logarithmic map. In this new space common vector valued approaches can be applied. The final result is obtained by mapping the transformed symmetric matrices back onto the space of positive definite matrices using the matrix exponential map. However, the log-Euclidean metric is not affine invariant. As a consequence the approach might suffer from a change of coordinates. However, the formulation of anisotropic diffusion for tensor valued data based on the log-Euclidean metric might be a computational efficient alternative not proposed in literature so far. In [22,29] a Riemannian framework based on local coordinates has been proposed (see also in [30] for a variational framework for general manifolds). Although, the authors in [22,29] consider the affine invariant metric their approach may only be classified as intrinsic in a continuous formulation. For computing discrete data, a simple finite difference approximation is applied. Inferring from a continuous formulation without a proof to a discrete approximation can be misleading as constraints holding in the continuous case may be relaxed by discretization. As a consequence, the proposed approaches not necessarily preserve positive definiteness of tensors (for a detailed discussion of this topic for scalar valued signals we refer to [2]). Furthermore, the approach of [29] shows no significant difference with the log Euclidean framework whereas our approach clearly outperforms it. We refer to our approach as the full intrinsic scheme in order to distinguish it from schemes that are only intrinsic in the continuous setting. Anisotropic diffusion based on an extrinsic view [12,31] and by means of the exponential map [6] has been proposed. In both cases the Euclidian metric is used to measure distances between tensors. As a consequence, both approaches suffer from the eigenvalue swelling effect.

Our contribution. We derive an intrinsic anisotropic diffusion equation for the manifold of positive definite tensors. To this end, second order derivatives in the continuous as well as discrete approximations are derived as they occur in the anisotropic diffusion equation. The derived numerical scheme could also be used to generalize other PDEs involving mixed derivatives from scalar valued images to the manifold $P(n)$ without the need of local coordinates. In the experimental part, we provide a study in which we compare different state of the art regularization approaches with our approach.

2 Diffusion for Scalar Valued Images

We review diffusion filtering which is a well established image processing technique for scalar valued images [3,32,2]. We formulate the diffusion equation by means of a gradient descent of some energy functional that later allows us to generalize this concept to tensor valued data. Let f be a scalar valued image defined on a N-dimensional domain. Diffusion filtering image processing creates a family of images $\{u(x,t)|t \geq 0\}$ from the solution of the physical diffusion equation

$$\partial_t u = \operatorname{div}\left(\mathbf{D}\nabla u\right) \tag{1}$$

with initial condition $f = u(x,0)$ and diffusion tensor $\mathbf{D}$ with components d_{ij}. Note that we could also formulate the image restoration task as a solution of a diffusion reaction equation by adding a data depending term to (1). We will discuss the pure diffusion process only. All following results keep valid also for a formulation with data depending reaction terms. The diffusion equation can be reformulated applying the chain rule in the form $\partial_t u = \sum_{i,j}(\partial_i d_{ij})(\partial_j u) + d_{ij}\partial_i\partial_j u$ which will be more convenient for the formulation on tensor valued data. The diffusion process can be classified according to the diffusion tensor $\mathbf{D}$. If the diffusion tensor does not depend upon the evolving image, the diffusion process is denoted as *linear* due to the linearity of (1) otherwise it is termed *nonlinear*. The diffusion process can furthermore be classified into *isotropic* when the diffusion tensor is proportional to the identity matrix otherwise it is denoted as *anisotropic*. Except for the nonlinear anisotropic diffusion scheme, the diffusion equation can be derived from a corresponding energy functional $E(u)$ via calculus of variation, i.e. the gradient descent scheme of these energy functionals can be identified with a diffusion equation. Let $L(u)$ denote the energy density such that $E(u) = \int L(u)\, d\mathbf{x}$, $w : \mathbb{R}^N \to \mathbb{R}$ a test function and ε a real valued variable. The functional derivative $\delta E := \frac{\delta E(u+\varepsilon w)}{\delta \varepsilon}\Big|_{\varepsilon=0}$ of an energy functional $E(u)$ can be written as

$$\delta E = \int \langle \nabla L(u), w \rangle_u \, d\mathbf{x} \ , \tag{2}$$

where $\nabla L(u)$ defines the gradient of the energy density and $\langle \nabla L(u), w \rangle_u$ denotes the scalar product of the energy density gradient $\nabla L(u)$ and the test function evaluated at $\mathbf{x}$. Note that w as well as $\nabla L(u)$ are elements of the tangent space at u which is the Euclidian space itself for scalar valued images. As we will see in Sect. 4, this formulation allows a direct generalization to the space of symmetric positive definite tensors. The gradient descent scheme of the energy functional leads to the diffusion equation in terms of the energy density

$$\partial_t u = -\nabla L(u) \ . \tag{3}$$

Let us now consider the linear anisotropic diffusion equation (1), i.e. $\mathbf{D}$ not depending on the evolving signal. The corresponding energy function is known to be

$$E(u) = \frac{1}{2} \int \nabla u^T \mathbf{D} \nabla u \, d\mathbf{x} \ . \tag{4}$$

The functional derivative of (4) can be brought into the form

$$\delta E(u) = \int \langle -\mathrm{div}\left(\mathbf{D}\nabla u\right), w \rangle_u \, d\mathbf{x} \tag{5}$$

assuming homogenous Neumann boundary conditions and applying Green's formula. Comparing (5) with (2) gives together with (3) the diffusion equation (1). Our objective is now to generalize the linear anisotropic diffusion process to the space of positive definite tensors by means of the energy functional formulation. The nonlinear anisotropic diffusion equation on $P(n)$, can then be deduced from the linear one.

3 The Space of Positive Definite Tensors

In the following we review the structure of the space of positive definite tensors $P(n)$ and introduce the differential geometric tools necessary for deriving anisotropic diffusion equations for $P(n)$. By introducing a basis, any tensor can be identified with its corresponding matrix representation $A \in \mathbb{R}^{n\times n}$. The space of $n \times n$ matrices constitutes a vector space embodied with a scalar product $\langle A, B\rangle = \mathrm{Tr}\left(A^T B\right)$, inducing the norm $||A|| = \sqrt{\langle A, A\rangle}$. However, tensors $\boldsymbol{\Sigma}$ frequently occurring in computer vision and image processing applications, e.g. covariance matrices and DT-MRI tensors, embody further structure on the space of tensors: they are symmetric $\boldsymbol{\Sigma}^T = \boldsymbol{\Sigma}$ and positive definite, i.e. it holds $x^T \boldsymbol{\Sigma} x > 0$ for all nonzero $x \in \mathbb{R}^n$. The approach to anisotropic diffusion presented here, measures distances between tensors by the length of the shortest path, the geodesic, with respect to $GL(n)$ (affine) invariant Riemannian metric on $P(n)$. This metric takes the nonlinear structure of $P(n)$ into account and it has demonstrated in several other application its superiority over the flat Euclidean matric [17,18,20,21,7,22]. Such an *intrinsic* treatment requires the formulation of $P(n)$ as a Riemannian manifold, i.e. each tangent space is equipped with an inner product that smoothly varies from point to point. A geodesic $\boldsymbol{\Gamma}_{\mathbf{X}}(t)$ parameterized by the 'time' t and going through the tensor $\boldsymbol{\Gamma}(0) = \boldsymbol{\Sigma}$ at time $t = 0$ is uniquely defined by its tangent vector $\mathbf{X}$ at $\boldsymbol{\Sigma}$. This allows one to describe each geodesic by a mapping from the subspace $\mathcal{A} = (t\mathbf{X})$, $t \in \mathbb{R}$ spanned by the tangent vector onto the manifold $P(n)$. The $GL(n)$ invariant metric is induced by the scalar product

$$\langle W_1, W_2\rangle_{\boldsymbol{\Sigma}} = \mathrm{Tr}\left(\boldsymbol{\Sigma}^{-\frac{1}{2}} W_1 \boldsymbol{\Sigma}^{-1} W_2 \boldsymbol{\Sigma}^{-\frac{1}{2}}\right) \ , \tag{6}$$

as one can easily verify. The $GL(n)$ invariant metric allows to derive an expression of the geodesic equation going through $\boldsymbol{\Sigma}$ by tangent vectors $\mathbf{X}$ [7]

$$\boldsymbol{\Gamma}_{\boldsymbol{\Sigma}}(t) = \boldsymbol{\Sigma}^{\frac{1}{2}} \exp(t\boldsymbol{\Sigma}^{-\frac{1}{2}} \mathbf{X} \boldsymbol{\Sigma}^{-\frac{1}{2}}) \boldsymbol{\Sigma}^{\frac{1}{2}} \ . \tag{7}$$

For $t = 1$ this map is denoted as the exponential map which is one to one in case of the space of positive definite tensors. Its inverse, denoted as the logarithmic map, reads

$$\mathbf{X} = \boldsymbol{\Sigma}^{\frac{1}{2}} \log\left(\boldsymbol{\Sigma}^{-\frac{1}{2}} \boldsymbol{\Gamma}_{\boldsymbol{\Sigma}}(1) \boldsymbol{\Sigma}^{-\frac{1}{2}}\right) \boldsymbol{\Sigma}^{\frac{1}{2}} \ . \tag{8}$$

As the gradient of any energy density ∇L is element of the tangent space [33], we can formulate a diffusion process as $\partial_t \boldsymbol{\Sigma} = -\nabla L$ on the tangent space. The evolution of the tensor $\boldsymbol{\Sigma}$ is obtained by going a small step in the negative direction of the gradient $-dt\nabla L$ and mapping this point back on the manifold using the geodesic equation (7). The energy density is then computed for the tangent vector at $\boldsymbol{\Gamma}_{\boldsymbol{\Sigma}}(dt)$ which in turn can then be used for finding the next tensor in the evolving scheme as described above. This is a gradient descent approach, denoted as the geodesic marching scheme, for energy densities defined on $P(n)$ and which per construction assures that we cannot leave the manifold.

4 Riemannian Anisotropic Diffusion

After reviewing the necessary differential geometric tools, we will derive anisotropic diffusion equations for a tensor field $P(n)$ over $\mathbb{R}^N$. As done for the diffusion equation for the scalar valued signals (Sect. 2), we derive the linear diffusion equation by variation of the corresponding energy functional and infer from the linear equation to the nonlinear counterpart. Let $\partial_i \boldsymbol{\Sigma}(\mathbf{x})$, $i = 1, ..., N$ denote partial derivative of the tensor field in direction i, elements of the tangent space at $\boldsymbol{\Sigma}$. We define the energy functional

$$E(\boldsymbol{\Sigma}) = \int \sum_{i,j} d_{ij} \langle \partial_i \boldsymbol{\Sigma}, \partial_j \boldsymbol{\Sigma} \rangle_{\boldsymbol{\Sigma}} \, d\mathbf{x} \tag{9}$$

$$\text{with} \quad \langle \partial_i \boldsymbol{\Sigma}, \partial_j \boldsymbol{\Sigma} \rangle_{\boldsymbol{\Sigma}} = \text{Tr}\left((\partial_i \boldsymbol{\Sigma}) \boldsymbol{\Sigma}^{-1} (\partial_j \boldsymbol{\Sigma}) \boldsymbol{\Sigma}^{-1} \right) \ . \tag{10}$$

The components of the diffusion tensor d_{ij} (please do not confuse d_{ij} with the elements of the tensor field) locally controls the direction of smoothing and for the moment being does not depend on the evolving tensor field. The gradient of the energy functional is then derived by defining a 'test function' W that is actually a tangent vector in the tangent space at $\boldsymbol{\Sigma}$ and computing the functional derivative

$$\delta E = 2 \int \sum_{ij} d_{ij} \text{Tr}((\partial_i W) \, \boldsymbol{\Sigma}^{-1} \, (\partial_j \boldsymbol{\Sigma}) \, \boldsymbol{\Sigma}^{-1} \tag{11}$$

$$- (\partial_i \boldsymbol{\Sigma}) \, \boldsymbol{\Sigma}^{-1} \, (\partial_j \boldsymbol{\Sigma}) \, \boldsymbol{\Sigma}^{-1} W \boldsymbol{\Sigma}^{-1}) \, d\mathbf{x} \tag{12}$$

In order to get rid of the derivatives on the 'test function' W we integrate by parts with respect to x_j. Assuming homogenous Neumann boundary conditions the functional derivative can be brought in the form

$$\delta E = -2 \sum_{i,j} \int \langle W, \boldsymbol{\Sigma} \partial_i (d_{ij} \boldsymbol{\Sigma}^{-1} (\partial_j \boldsymbol{\Sigma}) \boldsymbol{\Sigma}^{-1}) \boldsymbol{\Sigma} \tag{13}$$

$$+ (\partial_i \boldsymbol{\Sigma}) \boldsymbol{\Sigma}^{-1} (\partial_j \boldsymbol{\Sigma}) \rangle_{\boldsymbol{\Sigma}} \, d\mathbf{x} \tag{14}$$

Comparing the inner product with the general form in (2) identifies the gradient of the energy density

$$\nabla L = -2 \sum_{i,j} \boldsymbol{\Sigma} \partial_i (d_{ij} \boldsymbol{\Sigma}^{-1} (\partial_j \boldsymbol{\Sigma}) \boldsymbol{\Sigma}^{-1}) \boldsymbol{\Sigma} + (\partial_i \boldsymbol{\Sigma}) \boldsymbol{\Sigma}^{-1} (\partial_j \boldsymbol{\Sigma}) \ . \tag{15}$$

Inserting this energy density in (3) results in the desired diffusion equation. Using the identity $\partial_i \boldsymbol{\Sigma}^{-1} = -\boldsymbol{\Sigma}^{-1} (\partial_i \boldsymbol{\Sigma}) \boldsymbol{\Sigma}^{-1}$ the energy density gradient can be simplified to

$$\nabla L = -2 \sum_{i,j} \left(\partial_i \partial_j \boldsymbol{\Sigma} - (\partial_i \boldsymbol{\Sigma}) \boldsymbol{\Sigma}^{-1} (\partial_j \boldsymbol{\Sigma}) \right) - 2 \sum_{i,j} (\partial_i d_{ij}) (\partial_j \boldsymbol{\Sigma}) \tag{16}$$

The terms on the right side of (16) for which $i = j$ hold $\Delta_i \boldsymbol{\Sigma} = \partial_i^2 \boldsymbol{\Sigma} - (\partial_i \boldsymbol{\Sigma}) \boldsymbol{\Sigma}^{-1} (\partial_i \boldsymbol{\Sigma})$ are components of the Laplace Beltrami operator $\Delta = \sum_i \Delta_i$ derived in [7]. In addition to the work in [20,7], we also derived mixed components

$$\Delta_{ij} \boldsymbol{\Sigma} = \partial_i \partial_j \boldsymbol{\Sigma} - (\partial_i \boldsymbol{\Sigma}) \boldsymbol{\Sigma}^{-1} (\partial_j \boldsymbol{\Sigma}), \quad i \neq j \tag{17}$$

needed for the linear anisotropic diffusion equation. The nonlinear anisotropic diffusion equation is defined exchanging the diffusion tensor components in (4) with components depending on the evolved tensor field. So we have all components to define an anisotropic diffusion equation on the space of positive definite matrices in an intrinsic way. To this end, only the second order derivatives ∂_i^2 and $\partial_i \partial_j$ occurring in (1) need to be exchanged by their counterparts Δ_i and Δ_{ij}. So far we have not specified the explicit form of the diffusion tensor which should be made up here. We generalize the structure tensor to the nonlinear space and afterwards, as in the case of scalar valued images, construct the diffusion tensor from the spectral decomposition of the structure tensor. Let $\nabla \boldsymbol{\Sigma} = (\partial_1 \boldsymbol{\Sigma}, ..., \partial_N \boldsymbol{\Sigma})^T$ denote the gradient and $\mathbf{a}$ a unite vector in $\mathbb{R}^N$ such that we can express the derivative in direction $\mathbf{a}$ as $\partial_a = \mathbf{a}^T \nabla$. The direction of less variation in the tensor space can then analogous to the structure tensor in linear spaces, be estimated by minimizing the local energy

$$E(\mathbf{a}) = \int_V \langle \partial_a \boldsymbol{\Sigma}, \partial_a \boldsymbol{\Sigma} \rangle_{\boldsymbol{\Sigma}} d\mathbf{x} = \mathbf{a}^T J \mathbf{a} \ , \tag{18}$$

where we defined the components of the structure tensors J on $P(n)$ by $J_{ij} = \int_V \langle \partial_i \boldsymbol{\Sigma}, \partial_j \boldsymbol{\Sigma} \rangle_{\boldsymbol{\Sigma}} d\mathbf{x}$.The diffusion tensor $\mathbf{D}$ is then designed as usual by exchanging the eigenvalues λ_j of the structure tensor by a decreasing diffusivity function $g(\lambda_j)$. For our numerical experiments (in 2D) we choose $g(\lambda_l) = 1/\sqrt{1 + \lambda_l/\beta^2}$ for the larger eigenvalue and $g(\lambda_s) = 1$ for the smaller eigenvalue with the heuristically chosen contrast parameter $\beta = 0.05$.

5 Numerical Issues

So far we have assumed the tensor to be defined on a continuous domain. In the experiential setting we are confronted with tensor fields defined on a discrete grid. The application of Riemanian anisotropic diffusion requires a discrete approximation for the derivatives derived in Sect. 4. In principle, we could use matrix differences to approximate the derivatives but this would contradict our effort to derive an intrinsic expression of the anisotropic diffusion equation. The finite differences are extrinsic since they are based on Euclidian differences between tensors, i.e. they use the difference in the space of symmetric matrices and not the Riemannian metric of the space $P(n)$. In order to approximate the gradient ∇L in (16) on a discrete grid, we need discrete approximations of derivatives of first and second order. Intrinsic approximations to first order derivatives have already proposed in [20] and is reviewed here with the following preposition. Let us denote with $T\boldsymbol{\Sigma}_x^{e_j} := \overrightarrow{\boldsymbol{\Sigma}(x)\boldsymbol{\Sigma}(x+\varepsilon e_j)}$ the tangent vector defined by the logarithmic map as

$$T\boldsymbol{\Sigma}_x^{e_j} = \boldsymbol{\Sigma}^{\frac{1}{2}} \log\left(\boldsymbol{\Sigma}^{-\frac{1}{2}} \boldsymbol{\Sigma}(x+\varepsilon e_j) \boldsymbol{\Sigma}^{-\frac{1}{2}}\right) \boldsymbol{\Sigma}^{\frac{1}{2}} \tag{19}$$

Preposition 1. The first order discrete approximation of the first order derivative of $\boldsymbol{\Sigma}$ in direction j reads

$$\partial_j \boldsymbol{\Sigma} = \frac{1}{2\varepsilon}\left(\overrightarrow{\boldsymbol{\Sigma}(x)\boldsymbol{\Sigma}(x+\varepsilon e_j)} - \overrightarrow{\boldsymbol{\Sigma}(x)\boldsymbol{\Sigma}(x-\varepsilon e_j)}\right) + O(\varepsilon) \tag{20}$$

A second order discrete approximation scheme to the second order derivative in direction e_j has been derived in [7]. We state it here as a second preposition, for the proof see [7].

Preposition 2. The second order discrete approximation of the second order derivative in direction e_j is

$$\Delta_j \boldsymbol{\Sigma} = \frac{1}{\varepsilon^2}(\overrightarrow{\boldsymbol{\Sigma}(x)\boldsymbol{\Sigma}(x+\varepsilon e_j)} + \overrightarrow{\boldsymbol{\Sigma}(x)\boldsymbol{\Sigma}(x-\varepsilon e_j)}) + O(\varepsilon^2) \ . \tag{21}$$

For the anisotropic diffusion equation we also need mixed derivatives $\Delta_{ij}\boldsymbol{\Sigma}$ that can be approximated according to preposition 3.

Preposition 3. The second order discrete approximation of the second order mixed derivative in direction i and j is given by

$$\begin{aligned}\frac{\Delta_{ij}\boldsymbol{\Sigma} + \Delta_{ji}\boldsymbol{\Sigma}}{2} = \frac{1}{\varepsilon^2}(&\overrightarrow{\boldsymbol{\Sigma}(x)\boldsymbol{\Sigma}(x+\varepsilon e_n)} + \overrightarrow{\boldsymbol{\Sigma}(x)\boldsymbol{\Sigma}(x-\varepsilon e_n)} \\ &-\overrightarrow{\boldsymbol{\Sigma}(x)\boldsymbol{\Sigma}(x+\varepsilon e_p)} - \overrightarrow{\boldsymbol{\Sigma}(x)\boldsymbol{\Sigma}(x-\varepsilon e_p)}) + O(\varepsilon^2) \ ,\end{aligned} \tag{22}$$

with the abbreviation $e_n = \frac{1}{\sqrt{2}}(e_i + e_j)$, $e_p = \frac{1}{\sqrt{2}}(e_i - e_j)$.

Proof. We expend the tangent vector as

$$T\boldsymbol{\Sigma}_x^{e_n} = \varepsilon\partial_n\boldsymbol{\Sigma} + \frac{\varepsilon^2}{2}\partial_n^2\boldsymbol{\Sigma} - \frac{\varepsilon^2}{2}(\partial_n\boldsymbol{\Sigma})\boldsymbol{\Sigma}^{-\frac{1}{2}}(\partial_n\boldsymbol{\Sigma}) + O(\varepsilon^3) \ . \tag{23}$$

Now, we express the derivative in direction n by derivatives along the coordinate axes in i and j direction , $\partial_n = \frac{1}{\sqrt{2}}\partial_i + \frac{1}{\sqrt{2}}\partial_j$, yielding

$$\begin{aligned}T\boldsymbol{\Sigma}_x^{e_n} = &\frac{\varepsilon}{\sqrt{2}}(\partial_i\boldsymbol{\Sigma} + \partial_j\boldsymbol{\Sigma}) + \frac{\varepsilon^2}{4}(\big(\partial_i^2\boldsymbol{\Sigma} + \partial_j^2\boldsymbol{\Sigma} + 2\partial_i\partial_j\boldsymbol{\Sigma}\big) \\ &-(\partial_i\boldsymbol{\Sigma})\boldsymbol{\Sigma}^{-\frac{1}{2}}(\partial_i\boldsymbol{\Sigma}) - (\partial_j\boldsymbol{\Sigma})\boldsymbol{\Sigma}^{-\frac{1}{2}}(\partial_j\boldsymbol{\Sigma}) \\ &-(\partial_i\boldsymbol{\Sigma})\boldsymbol{\Sigma}^{-\frac{1}{2}}(\partial_j\boldsymbol{\Sigma}) - (\partial_j\boldsymbol{\Sigma})\boldsymbol{\Sigma}^{-\frac{1}{2}}(\partial_i\boldsymbol{\Sigma})) + O(\varepsilon^3) \ .\end{aligned}$$

Computing the sum $T\boldsymbol{\Sigma}_x^{\Delta e_n} := T\boldsymbol{\Sigma}_x^{e_n} + T\boldsymbol{\Sigma}_x^{-e_n}$ becomes a fourth order approximation as all uneven terms cancel out

$$\begin{aligned}T\boldsymbol{\Sigma}_x^{\Delta e_n} = &\frac{\varepsilon^2}{4}(\big(\partial_i^2\boldsymbol{\Sigma} + \partial_j^2\boldsymbol{\Sigma} + 2\partial_i\partial_j\boldsymbol{\Sigma}\big) - (\partial_i\boldsymbol{\Sigma})\boldsymbol{\Sigma}^{-\frac{1}{2}}(\partial_i\boldsymbol{\Sigma}) - \\ &(\partial_j\boldsymbol{\Sigma})\boldsymbol{\Sigma}^{-\frac{1}{2}}(\partial_j\boldsymbol{\Sigma}) - (\partial_i\boldsymbol{\Sigma})\boldsymbol{\Sigma}^{-\frac{1}{2}}(\partial_j\boldsymbol{\Sigma}) - (\partial_j\boldsymbol{\Sigma})\boldsymbol{\Sigma}^{-\frac{1}{2}}(\partial_i\boldsymbol{\Sigma})) + O(\varepsilon^4)\end{aligned} \tag{24}$$

Expanding $T\boldsymbol{\Sigma}_x^{\Delta e_p} := T\boldsymbol{\Sigma}_x^{e_p} + T\boldsymbol{\Sigma}_x^{-e_p}$ in the same way yields

$$\begin{aligned}T\boldsymbol{\Sigma}_x^{\Delta e_p} = &\frac{\varepsilon^2}{4}(\big(\partial_i^2\boldsymbol{\Sigma} + \partial_j^2\boldsymbol{\Sigma} - 2\partial_i\partial_j\boldsymbol{\Sigma}\big) - (\partial_i\boldsymbol{\Sigma})\boldsymbol{\Sigma}^{-\frac{1}{2}}(\partial_i\boldsymbol{\Sigma}) - \\ &(\partial_j\boldsymbol{\Sigma})\boldsymbol{\Sigma}^{-\frac{1}{2}}(\partial_j\boldsymbol{\Sigma}) + (\partial_i\boldsymbol{\Sigma})\boldsymbol{\Sigma}^{-\frac{1}{2}}(\partial_j\boldsymbol{\Sigma}) + (\partial_j\boldsymbol{\Sigma})\boldsymbol{\Sigma}^{-\frac{1}{2}}(\partial_i\boldsymbol{\Sigma})) + O(\varepsilon^4)\end{aligned} \tag{25}$$

By subtracting (25) from (24) and dividing the square of the grid size ε^2 we obtained the claimed second order approximation for the mixed derivatives which concludes the proof.

6 Experiments

Performance of our Riemannian anisotropic diffusion (RAD) approach is demonstrated on synthetic tensor fields and real DT-MRI data. We compare our Riemannian anisotropic diffusion scheme with three state of the art tensor valued regularization schemes: the anisotropic diffusion (EAD) scheme based on the flat Euclidean metric [12,31], the intrinsic nonlinear isotropic diffusion (RID) scheme [20] and the nonlinear isotropic diffusion (LEID) scheme based on the log-Euclidean metric [34]. As a computational effective alternative to our Riemannian anisotropic diffusion scheme, we propose to combine the diffusion scheme proposed in [12,31] with the log-Euclidean metric [34] which is considered as a fourth reference method (LEAD). As a performance measure for the regularized tensor field, we choose the fractional anisotropy (FA) [35]. Measures derived from DT-MRI such as the FA are used to generate additional image contrast required for detection of brain lesions, or to delineate white matter (highly directional structures) from non-white matter tissue, which is important for surgery. FA takes on values between 0 (corresponding to perfect isotropy) and 1 indicating maximal anisotropy. For solving the diffusion equations, we used the same time step of $dt = 0.01$ for all experiments and computed the evolving tensor field for 1000 time steps. As shown in [21], the linear gradient descent scheme realizes a first order approximation to the intrinsic marching scheme, such that for small time steps diffusion processes based on different metrics should be comparable for distinct times.

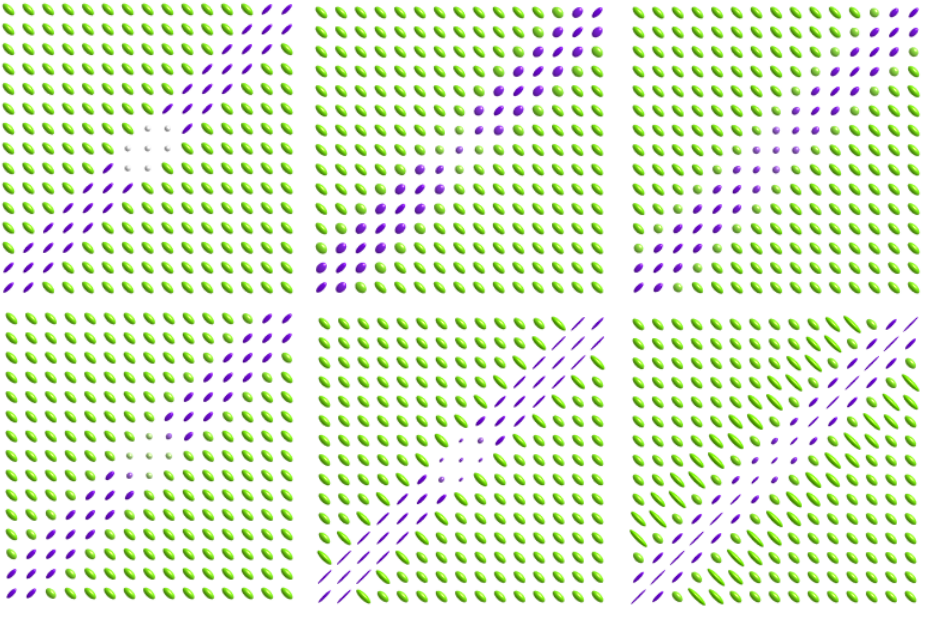

Fig. 1. Line reconstruction experiment; upper row (from left to right): original tensor field, EAD scheme, LEAD scheme; lower row (from left to right): LEID scheme, RID scheme, RAD scheme

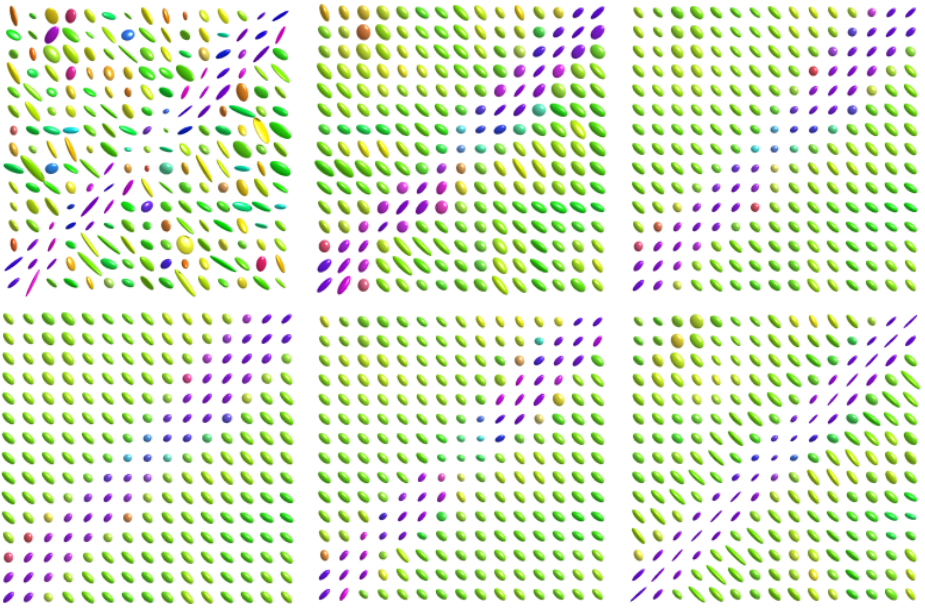

Fig. 2. Denoising experiment; upper row (from left to right): noise corrupted tensor field, EAD scheme, our LEAD scheme; lower row (from left to right): LEID scheme, RID scheme, RAD scheme

6.1 Synthetic Data

Experiment 1. In the first experiment on synthetic data we examine the ability of the different diffusion processes to complete interrupted line structures. To this end, we generate a 32×32 large tensor field of 3×3 tensors (see Fig. 2 upper left; in order to visualize details more precise only a cutout of the tensor field is shown). Each tensor is represented by an ellipsoid and the orientation of its main axis is additional color coded whereas the FA is encoded in the saturation of the depicted tensors. The line structure is interrupted by isotropic tensors with small eigenvalues ($\lambda_j = 0.05$) that are hardly visible due to the saturation encoding of the FA. The results for all diffusion processes are shown in Fig. 1. The nonlinear isotropic processes LEID and RID stops at the line interruption and is not able to complete the line. This results from the fact that, although the smoothing process is also anisotropic for nonlinear isotropic diffusion processes [20], the diffusivity function depends only on its direct neighbors and therefore does not 'see' the line behind the gap. The anisotropic diffusion schemes are steered by the diffusion tensor which encodes the directional information of a neighborhood depending on the average region for the structure tensor. The anisotropic diffusion approaches fill the gap and reconstruct the line. However, again the EAD-process suffers from the eigenvalue swelling effect and only one tensor connects both interrupted line structures. However increasing the average region of the structure tensor might fill the gap more clearly. Our RAD and LEAD schemes reconstruct the line structure. However, we observe a small

decreasing of the anisotropy for the log-Euclidean metric, whereas the anisotropy for the affine invariant metric increases in the vicinity of image borders.

Experiment 2. In this experiment we examine the ability of the different diffusion schemes to reconstruct the tensor field from noisy data. To this end, we corrupt the tangent vector of each tensor by Gaussian noise (with standard deviations $\sigma = 0.6$). Fig. 2 shows the noise corrupted field (the noise free tensor field is the same as in experiment 1) and the evolved tensor fields for the different diffusion schemes. The anisotropic schemes manage (more or less) to close the gap in the line structure despite the noise whereas the isotropic schemes does not. The schemes based on the log Euclidean metric lead to a slight decrease of the anisotropy whereas the RAD schemes leads to an increase of the anisotropy in the tensor field. How this effect influences further processing steps, e.g. fiber tracking algorithm, is left to be examined for future research.

6.2 Real Data

Experiment 3. In our last experiment, the different algorithms were applied to DT-MRI data measured from a *human* brain *in-vivo*. DT-MRI of the brain of a healthy volunteer (written informed consent was obtained) was performed on a 1.5 T Magnetom Avanto scanner (Siemens Medical Solutions). A single-shot diffusion-weighted twice-refocused spin-echo planar imaging sequence was used. Measurement parameters were

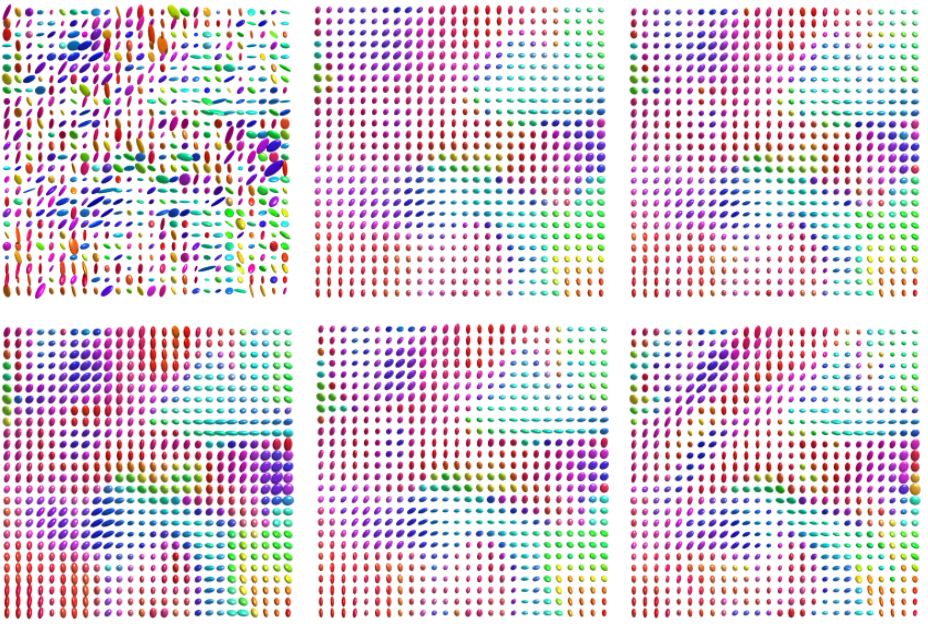

Fig. 3. Denoising experiment 3; (upper row, from left to right): noisy DT-MRI image, LEID scheme, RID scheme; (lower row, from left to right) EAD scheme, LEAD scheme, RAD scheme

as follows : TR = 6925 ms / TE=104ms / 192 matrix with 6/8 phase partial fourier, 23 cm field of view (FOV), and 36 2.4-mm-thick contiguous axial slices. The in-plane resolution was 1.2 mm/pixel. We estimate a volumetric tensor field of size $192 \times 192 \times 36$ and take one slice for further processing. For evaluation purposes we recorded tensor fields of the brain with 6 different signal-to-noise ratios (SNR), denoted as DTI1-6 in the following. Thus, we can use the DT-MRI-images (DTI6) from the long measurement (i.e. good SNR) as a reference data set, where we compare the FA of the tensor with the results obtained from the lower SNR data set (DTI1-5), which can be obtained in a clinical feasible measurement time. We compute, starting from the five different noisy tensor fields, the evolved tensor fields for all considered diffusion schemes (Fig. 3 shows cutouts of the noisy field and evolved fields) and compare its FA with the reference field. All schemes lead to rather smooth tensor fields. However, the anisotropic diffusion schemes (EAD, LEAD and RAD) lead to an enhancement of orientated structures within in the tensor fields which is most distinct for our RAD scheme. As in the previous experiments, the eigenvalue swelling effect in case of the EAD scheme can be observed. Our RAD/LEAD schemes yield the best results among anisotropic regularization schemes with respect to the FA measure as shown in Tab. 1.

Table 1. Results of experiment 3: The average and standard deviation of the the fractional anisotropy error $|FA - \underline{FA}|$ (FA belongs to the reference tensor field) over 1000 time steps for each diffusion scheme as well as for five different noise levels are computed

Method	DTI1	DTI2	DTI3	DTI4	DTI5
EAD	0.098 ± 0.007	0.100 ± 0.008	0.103 ± 0.008	0.109 ± 0.009	0.112 ± 0.010
RID	0.112 ± 0.016	0.119 ± 0.015	0.116 ± 0.013	0.114 ± 0.012	0.113 ± 0.013
LEID	0.099 ± 0.017	0.108 ± 0.017	0.107 ± 0.014	0.106 ± 0.012	0.105 ± 0.012
LEAD	$\mathbf{0.078 \pm 0.005}$	$\mathbf{0.079 \pm 0.006}$	$\mathbf{0.081 \pm 0.006}$	$\mathbf{0.084 \pm 0.007}$	$\mathbf{0.086 \pm 0.007}$
RAD	$\mathbf{0.089 \pm 0.004}$	$\mathbf{0.089 \pm 0.005}$	$\mathbf{0.093 \pm 0.007}$	$\mathbf{0.096 \pm 0.007}$	$\mathbf{0.098 \pm 0.009}$

7 Conclusion

We generalized the concept of anisotropic diffusion to tensor valued data with respect to the affine invariant Riemannian metric. We derived the intrinsic mixed second order derivatives as they are required for the anisotropic diffusion process. Furthermore, we derived a discrete intrinsic approximation scheme for the mixed second order derivatives. Since mixed second order derivatives appear also in other methods based on partial differential equation, this contribution could also serve as a basis for generalizing these methods in an intrinsic way in a discrete formulation. Experiments on synthetic as well as real world data demonstrate the value of our full intrinsic differential geometrical formulation of the anisotropic diffusion concept. As a computational effective alternative, we proposed an anisotropic diffusion scheme based on the log-Euclidean metric. Summing up, our proposed anisotropic diffusion schemes show promising results on the given test images. Further work might examine the reconstruction properties of other tensor characteristics as well as the influence on so far heuristically chosen parameters, e.g. the diffusivity function.

References

1. Berger, M.-O., Deriche, R., Herlin, I., Jaffré, J., Morel, J.-M. (eds.): Icaos 1996: Images and wavelets and PDEs. Lecture Notes in Control and Information Sciences, vol. 219 (1996)
2. Weickert, J.: Anisotropic diffusion in image processing. Teubner, Stuttgart (1998)
3. Perona, P., Malik, J.: Scale-space and edge detection using anisotropic diffusion. IEEE Transactions on Pattern Analysis and Machine Intelligence 12 (1990)
4. Bigün, J., Granlund, G.H.: Optimal orientation detection of linear symmetry. In: ICCV, London, UK, pp. 433–438 (1987)
5. Tschumperlé, D., Deriche, R.: Diffusion tensor regularization with constraints preservation. In: Proc. IEEE Computer Society Conference on Computer Vision and Pattern Recognition (CVPR 2001), pp. 948–953 (2001)
6. Chefd'hotel, C., Tschumperlé, D., Deriche, R., Faugeras, O.: Regularizing flows for constrained matrix-valued images. J. Math. Imaging Vis. 20(1-2), 147–162 (2004)
7. Pennec, X., Fillard, P., Ayache, N.: A Riemannian framework for tensor computing. International Journal of Computer Vision 66(1), 41–66 (2006)
8. Castano-Moraga, C.A., Lenglet, C., Deriche, R., Ruiz-Alzola, J.: A Riemannian approach to anisotropic filtering of tensor fields. Signal Processing 87(2), 263–276 (2007)
9. Weickert, J., Hagen, H.: Visualization and Processing of Tensor Fields (Mathematics and Visualization). Springer, New York (2005)
10. Rao, C.: Information and accuracy attainable in estimation of statistical parameters. Bull. Calcutta Math. Soc. 37, 81–91 (1945)
11. Martin-Fernandez, M., San-Jose, R., Westin, C.F., Alberola-Lopez, C.: A novel Gauss-Markov random field approach for regularization of diffusion tensor maps. In: Moreno-Díaz Jr., R., Pichler, F. (eds.) EUROCAST 2003. LNCS, vol. 2809, pp. 506–517. Springer, Heidelberg (2003)
12. Weickert, J., Brox, T.: Diffusion and regularization of vector- and matrix-valued images. In: Inverse Problems, Image Analysis, and Medical Imaging. Contemporary Mathematics, pp. 251–268 (2002)
13. Westin, C.-F., Knutsson, H.: Tensor field regularization using normalized convolution. In: Moreno-Díaz Jr., R., Pichler, F. (eds.) EUROCAST 2003. LNCS, vol. 2809, pp. 564–572. Springer, Heidelberg (2003)
14. Burgeth, B., Didas, S., Florack, L., Weickert, J.: A generic approach to the filtering of matrix fields with singular PDEs. In: Sgallari, F., Murli, A., Paragios, N. (eds.) SSVM 2007. LNCS, vol. 4485, pp. 556–567. Springer, Heidelberg (2007)
15. Gur, Y., Sochen, N.A.: Denoising tensors via Lie group flows. In: Paragios, N., Faugeras, O., Chan, T., Schnörr, C. (eds.) VLSM 2005. LNCS, vol. 3752, pp. 13–24. Springer, Heidelberg (2005)
16. Moakher, M.: A differential geometric approach to the geometric mean of symmetric positive-definite matrices. SIAM J. Matrix Anal. Appl (2003)
17. Fletcher, P., Joshi, S.: Principle geodesic analysis on symmetric spaces: Statistics of diffusion tensors. In: Computer Vision and Mathematical Methods in Medical and Biomedical Image Analysis, ECCV 2004 Workshops CVAMIA and MMBIA, pp. 87–98 (2004)
18. Lenglet, C., Rousson, M., Deriche, R., Faugeras, O.D., Lehericy, S., Ugurbil, K.: A Riemannian approach to diffusion tensor images segmentation. In: Christensen, G.E., Sonka, M. (eds.) IPMI 2005. LNCS, vol. 3565, pp. 591–602. Springer, Heidelberg (2005)
19. Batchelor, P.G., Moakher, M., Atkinson, D., Calamante, F., Connelly, A.: A rigorous framework for diffusion tensor calculus. Magn. Reson. Med. 53(1), 221–225 (2005)
20. Fillard, P., Arsigny, V., Ayache, N., Pennec, X.: A Riemannian framework for the processing of tensor-valued images. In: Fogh Olsen, O., Florack, L.M.J., Kuijper, A. (eds.) DSSCV 2005. LNCS, vol. 3753, pp. 112–123. Springer, Heidelberg (2005)

21. Lenglet, C., Rousson, M., Deriche, R., Faugeras, O.: Statistics on the manifold of multivariate normal distributions: Theory and application to diffusion tensor MRI processing. J. Math. Imaging Vis. 25(3), 423–444 (2006)
22. Zéraï, M., Moakher, M.: Riemannian curvature-driven flows for tensor-valued data. In: Sgallari, F., Murli, A., Paragios, N. (eds.) SSVM 2007. LNCS, vol. 4485, pp. 592–602. Springer, Heidelberg (2007)
23. Helgason, S.: Differential Geometry, Lie groups and symmetric spaces. Academic Press, London (1978)
24. El-Fallah, A., Ford, G.: On mean curvature diffusion in nonlinear image filtering. Pattern Recognition Letters 19, 433–437 (1998)
25. Sochen, N., Kimmel, R., Malladi, R.: A geometrical framework for low level vision. IEEE Transaction on Image Processing, Special Issue on PDE based Image Processing 7(3), 310–318 (1998)
26. Begelfor, E., Werman, M.: Affine invariance revisited. In: CVPR '06: Proceedings of the 2006 IEEE Computer Society Conference on Computer Vision and Pattern Recognition, pp. 2087–2094. IEEE Computer Society Press, Washington (2006)
27. Zhang, F., Hancock, E.: Tensor MRI regularization via graph diffusion. In: BMVC 2006, pp. 578–589 (2006)
28. Arsigny, V., Fillard, P., Pennec, X., Ayache, N.: Log-Euclidean metrics for fast and simple calculus on diffusion tensors. Magnetic Resonance in Medicine 56(2), 411–421 (2006)
29. Gur, Y., Sochen, N.A.: Fast invariant Riemannian DT-MRI regularization. In: Proc. of IEEE Computer Society Workshop on Mathematical Methods in Biomedical Image Analysis (MMBIA), Rio de Janeiro, Brazil, pp. 1–7 (2007)
30. Mémoli, F., Sapiro, G., Osher, S.: Solving variational problems and partial differential equations mapping into general target manifolds. Journal of Computational Physics 195(1), 263–292 (2004)
31. Brox, T., Weickert, J., Burgeth, B., Mrázek, P.: Nonlinear structure tensors. Revised version of technical report no. 113. Saarland University, Saarbrücken, Germany (2004)
32. Nielsen, M., Johansen, P., Olsen, O., Weickert, J. (eds.): Scale-Space 1999. LNCS, vol. 1682. Springer, Heidelberg (1999)
33. Maaß, H.: Siegel's Modular Forms and Dirichlet Series. Lecture notes in mathematics, vol. 216. Springer, Heidelberg (1971)
34. Arsigny, V., Fillard, P., Pennec, X., Ayache, N.: Fast and simple calculus on tensors in the log-Euclidean framework. In: Duncan, J.S., Gerig, G. (eds.) MICCAI 2005. LNCS, vol. 3749, pp. 115–122. Springer, Heidelberg (2005)
35. Bihan, D.L., Mangin, J.F., Poupon, C., Clark, C.A., Pappata, S., Molko, N., Chabriat, H.: Diffusion tensor imaging: Concepts and applications. Journal of Magnetic Resonance Imaging 13(4), 534–546 (2001)